Non-Fermi-Liquid Behavior in Metallic Quasicrystals with Local Magnetic Moments

Eric C. Andrade,[1] Anuradha Jagannathan,[2] Eduardo Miranda,[3] Matthias Vojta,[4] and Vladimir Dobrosavljević[5]
[1]*Instituto de Física Teórica, Universidade Estadual Paulista, Rua Dr. Bento Teobaldo Ferraz, 271—Bloco II, 01140-070 São Paulo, SP, Brazil*
[2]*Laboratoire de Physique des Solides, CNRS-UMR 8502, Université Paris-Sud, 91405 Orsay, France*
[3]*Instituto de Física Gleb Wataghin, Unicamp, Rua Sérgio Buarque de Holanda, 777, CEP 13083-859 Campinas, SP, Brazil*
[4]*Institut für Theoretische Physik, Technische Universität Dresden, 01062 Dresden, Germany*
[5]*Department of Physics and National High Magnetic Field Laboratory, Florida State University, Tallahassee, Florida 32306, USA*
(Received 19 December 2014; published 14 July 2015)

Motivated by the intrinsic non-Fermi-liquid behavior observed in the heavy-fermion quasicrystal $Au_{51}Al_{34}Yb_{15}$, we study the low-temperature behavior of dilute magnetic impurities placed in metallic quasicrystals. We find that a large fraction of the magnetic moments are not quenched down to very low temperatures T, leading to a power-law distribution of Kondo temperatures $P(T_K) \sim T_K^{\alpha-1}$, with a nonuniversal exponent α, in a remarkable similarity to the Kondo-disorder scenario found in disordered heavy-fermion metals. For $\alpha < 1$, the resulting singular $P(T_K)$ induces non-Fermi-liquid behavior with diverging thermodynamic responses as $T \to 0$.

DOI: 10.1103/PhysRevLett.115.036403 PACS numbers: 71.10.Hf, 71.23.Ft, 75.20.Hr

Introduction.—Fermi-liquid (FL) theory forms the basis of our understanding of interacting fermions. It works in a broad range of systems, from weakly correlated metals [1] to strongly interacting heavy fermions [2]. Over the past decades, however, the properties of numerous metals have been experimentally found to deviate from FL predictions [3,4], and much effort has been devoted to the understanding of such non-Fermi-liquid (NFL) behavior. One interesting avenue is provided by quantum critical points (QCPs): NFL physics may occur in the associated quantum critical regime which is reached upon tuning the system via a nonthermal control parameter such as pressure, doping, or magnetic field [5,6].

Remarkably, recent experiments have provided compelling evidence of NFL behavior without fine-tuning in the heavy-fermion *quasicrystal* $Au_{51}Al_{34}Yb_{15}$ [7,8]. Furthermore, Ref. [7] also reports that no NFL behavior emerges when one considers a crystalline approximant instead of the quasicrystal, suggesting that this NFL regime is associated with the particular electronic states present in the quasicrystal but not in the approximant [9–14]. Conventional QCP approaches have been employed to explain the fascinating behavior in this alloy [15,16], but they consider the effects of a quasicrystalline environment of the conduction electrons only minimally.

In this work we intend to close this gap by presenting a detailed calculation of the fate of isolated localized magnetic moments when placed in both two- and three-dimensional quasicrystals. Our results for dilute impurities show that a considerable fraction of impurity moments is not quenched down to very low temperatures, leading to a power-law distribution of Kondo temperatures, $P(T_K) \propto T_K^{\alpha-1}$, with a nonuniversal exponent α. This results in NFL behavior in both χ and C/T as $T \to 0$: $\chi \sim C/T \sim T^{\alpha-1}$ [17], a scenario very reminiscent of the Kondo effect in disordered metals [18–23]. Moreover, we show that the strong energy dependence of the electronic density of states (DOS) characteristic of a quasicrystal leads to a situation such that small changes in the model parameters (band filling, Kondo coupling, etc.) may drive the system in and out of the NFL region.

Quasicrystalline wave functions.—A quasicrystal exhibits a small set of local environments, which reappear again and again, albeit not in a periodic fashion. Their pattern is not random either, since the structure factor shows sharp Bragg peaks, although their symmetry is noncrystallographic [24]. The n-fold symmetries (with values of $n = 5, 8, 10, \ldots$) seen in the diffraction pattern of quasicrystals arise due to the fact that the local environments occur with n equiprobable orientations.

The structure factor of quasicrystals is densely filled in reciprocal space with diffraction spots [24] of widely differing intensities. The brighter peaks are expected to lead to strong scattering of conduction electrons, giving rise to spikes in the DOS [25,26]. The scattering due to the remaining peaks, while weaker, results in wave functions which show fluctuations at all length scales. The Fibonacci chain, a one-dimensional quasicrystal, provides an example of such wave functions [9], often referred to as *critical* [9–13], in analogy with those found at the Anderson metal-insulator transition [27,28].

Tiling model.—For simplicity, we consider models on quasiperiodic tilings. We first report results obtained for a 2D tiling, where it is easier to handle large system sizes numerically. In the Supplemental Material [29], we show calculations for a 3D tiling [40] with very similar results, confirming that our scenario is independent of both tiling details and dimensionality.

The 2D tiling we consider is the octagonal tiling (Ammann-Beenker) [41], Fig. 1(a). This tiling is composed of two types of decorated tiles: squares and 45° rhombuses, which combine to create six distinct local environments with coordination number $z = 3, \ldots, 8$, Fig. 1(b).

As a minimal model to describe the electronic properties of quasicrystals, we consider a nearest-neighbor tight-binding Hamiltonian in standard notation

$$\mathcal{H}_c = -t \sum_{\langle ij \rangle, \sigma} (c^\dagger_{i\sigma} c_{j\sigma} + c^\dagger_{j\sigma} c_{i\sigma}). \quad (1)$$

In the following, energies are measured in units of t. In our calculation, we consider periodic approximants of the octagonal tiling of sizes $N_a = 7$, 41, 239, 1393, and 8119, obtained by the standard method of projecting down from a higher dimensional cubic lattice, as in previous works [41–44]. To reduce finite-size effects we use twisted boundary conditions, i.e., $\psi(\vec{r} + L\hat{x} + L\hat{y}) = e^{i\phi_x} e^{i\phi_y} \psi(\vec{r})$ for a sample of linear size L. Our final answer is obtained averaging over N_ϕ twist angles [45].

In Fig. 1(c) we show the well-known total DOS for the octagonal tiling $\langle \rho_c(\omega) \rangle = \sum_{i=1}^{N_a} \rho_i^c(\omega)/N_a$, with the local DOS at site i given by $\rho_i^c(\omega) = \overline{\sum_\nu |\psi_\nu^c(i)|^2 \delta(\omega - E_\nu^c)}$, where ψ_ν^c is an eigenstate of $\mathcal{H}_c$ in (1) with energy E_ν^c and the overline denotes the average over boundary conditions. $\langle \rho_c(\omega) \rangle$ has a strong energy dependence with several spikes and a pronounced dip at $\omega \approx \pm 2.0t$. The large peak at $\omega = 0$ is due to families of strictly localized states, a consequence of the local topology of the octagonal tiling [12,46]. The spatial structure of $\rho_i^c(\omega)$ is discussed in Ref. [29], where we show that it is well described by a log-normal distribution.

Local moments and large-N solution.—We now move to the main topic of this Letter: the investigation of the single-impurity Kondo effect in a metallic quasicrystal. Specifically, we consider the $U \to \infty$ Anderson impurity model

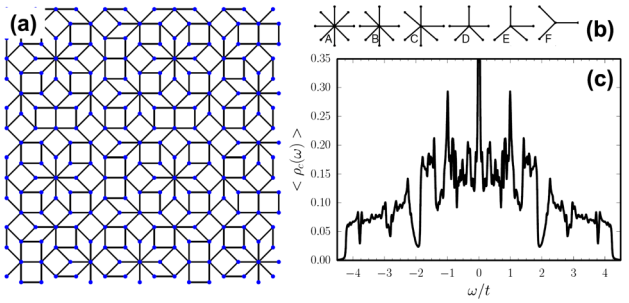

FIG. 1 (color online). Quasicrystal geometrical and electronic properties. (a) Square approximant for the perfect octagonal tiling with $N_a = 239$ sites. (b) The six local site environments with $z = 3, \ldots, 8$ nearest neighbors. (c) The total DOS as a function of the energy for the $N_a = 8119$ approximant averaged over $N_\phi = 64$ twist angles.

$$\mathcal{H} = \mathcal{H}_c + E_f \sum_\sigma n_{f\sigma} + V \sum_\sigma (f^\dagger_{\ell\sigma} c_{\ell\sigma} + c^\dagger_{\ell\sigma} f_{\ell\sigma}). \quad (2)$$

This model describes a band of noninteracting electrons (c band) which hybridize with a localized f orbital located at site ℓ. The operator $f^\dagger_{\ell\sigma}(f_{\ell\sigma})$ creates (destroys) an electron with spin σ at the impurity site ℓ and the $U \to \infty$ limit imposes the constraint $n_{f\sigma} = f^\dagger_{\ell\sigma} f_{\ell\sigma} \leq 1$. E_f is the f-level energy, measured with respect to the chemical potential μ, and the hybridization V couples the impurity site to the conduction band. To obtain quantitative results, we now turn to a large-N limit of Eq. (2) that allows us to access arbitrary values of the model parameters [47–49]. It introduces two variational parameters Z_ℓ (quasiparticle weights) and $\tilde{\varepsilon}_{f\ell}$ (renormalized f-energy levels), which are site dependent in the case of a quasicrystal. These parameters are determined by minimization of the saddle-point free energy (see [29] for further details)

$$F^\ell_{MF} = \frac{2}{\pi} \int_{-\infty}^{+\infty} f(\omega) \mathrm{Im}[\ln(\tilde{G}^f_\ell(\omega))] d\omega + (\tilde{\varepsilon}_{f\ell} - E_f)(Z_\ell - 1), \quad (3)$$

where $f(\omega)$ is the Fermi-Dirac distribution function. The quasiparticle f-level Green's function is given by $\tilde{G}^f_\ell(\omega) = [\omega - \tilde{\varepsilon}_f - Z_\ell \Delta_{f\ell}(\omega)]^{-1}$, with the f-electron hybridization function given by $\Delta_{f\ell}(\omega) = V^2 G^c_{\ell\ell}(\omega)$, where $G^c_{\ell\ell}(\omega) = \overline{\sum_\nu |\psi^c_\nu(\ell)|^2/(\omega - E^c_\nu)}$ is the c-electron Green's function. We define T_K as the (half-)width of the resonance at the Fermi level $T^\ell_K \equiv Z_\ell \mathrm{Im}[\Delta_{f\ell}(0)]$ [50] and introduce the Kondo coupling $J \equiv 2V^2/|E_f|$. The f-level occupation is simply given by $n_{f\ell} = 1 - Z_\ell$.

Because each site in the quasicrystal "sees" a different environment, encoded in $\Delta_{f\ell}(\omega)$, we numerically solve Eq. (3), at $T = 0$, individually placing Kondo impurities at all N_a sites of the approximant. Therefore, for every single impurity problem we obtain a different value of T_K, which we use to construct the distribution of the Kondo temperatures $P(T_K)$.

Power-law distribution of Kondo temperatures.—For Kondo impurities placed in a disordered metal [18–23] it is well established that the distribution of Kondo temperatures possesses a power-law tail at low T_K: $P(T_K) \propto T_K^{\alpha-1}$, with a nonuniversal exponent α [51]. For $\alpha < 1$, $P(T_K)$ becomes singular, and NFL behavior emerges in the system [17,29].

Surprisingly, we observe the same phenomenology for quasicrystals, with sample results shown in Fig. 2. Here we show the corresponding $P(T_K)$ for the octagonal tiling at $\mu = -2.2t$ as a function of T_K/T_K^{typ} (we defined the typical value of T_K as $T_K^{\mathrm{typ}} \equiv \exp[\langle \ln(T_K) \rangle]$). For approximants with $N_a \geq 239$ a clear power-law tail emerges for $T_K < T_K^{\mathrm{typ}}$ with an exponent which depends on the Kondo coupling J [29]. The dependence of T_K^{typ} on J is shown

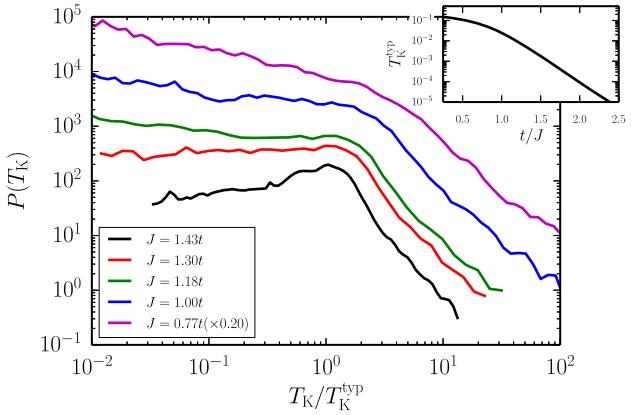

FIG. 2 (color online). Distribution of the local Kondo temperatures $P(T_K)$ on a log-log scale for several values of the Kondo coupling J; note that the curve corresponding to $J = 0.77t$ was scaled down. T_K on the horizontal axis has been normalized by T_K^{typ}; the unrenormalized distributions are shown in Ref. [29]. For $T_K \lesssim T_K^{typ}$ the distributions acquire a power-law form $P(T_K) \sim T_K^{\alpha-1}$, with the exponent α continuously varying with J. For $\alpha < 1$ the distribution is singular. [Notice that for $T_K \gtrsim T_K^{typ}$, $P(T_K)$ is also power-law like, with an exponent that does not depend on J. This is *not* the power-law regime we refer to in this work.] Inset: T_K^{typ} as a function of $1/J$ on a semilog scale. Here we considered $N_a = 1393$, $\mu = -2.2t$, and $N_\phi = 576$.

in the inset of Fig. 2, where we see that we obtain the expected exponential relation [2].

Given the strong energy variations of $\langle \rho_c(\omega) \rangle$, Fig. 1(c), it is then natural to ask whether the form $P(T_K) \propto T_K^{\alpha-1}$ is observed at different locations of the Fermi level μ. We checked that this is indeed the case: in Fig. 3 we show how the exponent α varies with J for several values of μ (to extract the value of α we followed Ref. [52]). The dashed straight lines correspond to the expected behavior at low J (Kondo limit) where we have $\alpha \propto J$ [29,51].

While the curves α vs J are all qualitatively the same, there are important features associated with the position of μ, and thus the value of $\langle \rho_c(0) \rangle$. Specifically for $\mu = -2.0t$ we enter the NFL region for relatively high values of the Kondo coupling, $J \simeq 2.35t$, and with an average f-level occupation $\langle n_f \rangle \simeq 0.89$ not so close to unity (for all the other values of μ considered $\langle n_f \rangle \simeq 1$). Moreover, for $J = 2.2t$ the thermodynamic properties diverge as a power law with an exponent $1 - \alpha \simeq 0.4$, but if we then vary μ by 10% we get $\alpha \gg 1$ and the system displays FL behavior.

To understand how a power-law distribution of Kondo temperatures emerges in this problem, we closely follow the arguments of Ref. [51]. In the Kondo limit, $\langle n_f \rangle \to 1$ and $J \to 0$, it is easy to show that $T_K^\ell = T_K^0 \exp[-\theta_\ell^2]$, where $\theta_\ell^2 = \pi \Delta'_{c\ell}(0)^2 / J \langle \Delta''_{c\ell}(0) \rangle$ and $T_K^0 = D \exp[-\pi \langle \Delta''_{c\ell}(0) \rangle / J]$ [29]. Here D is an energy cutoff and $\Delta_{c\ell}(\omega) \equiv \omega - 1/G^c_{\ell\ell}(\omega)$ is the local c-electron cavity function [53] with a single (double) prime denoting its real (imaginary) part. For $\Delta'_{c\ell}(0)$ distributed according to a Gaussian (see the inset of Fig. 3), it then follows immediately that, up to logarithmic corrections, $P(T_K) \propto T_K^{\alpha-1}$, with $\alpha = J \langle \Delta''_c(0) \rangle / 2\pi\sigma_c^2$, where σ_c is the variance of $P[\Delta'_c(0)]$ [29]. Physically, $\Delta'_{c\ell}(0)$ can be interpreted as a renormalized on-site site energy for the c electrons. The simple Gaussian form of $P[\Delta'_c(0)]$, as in the usual disordered problem [51], suggests an effective self-averaging, in the sense that for local quantities like $\Delta'_c(0)$ there seems to be no important distinction between disorder and quasiperiodic order. Nevertheless, we know that this surprising result *cannot* hold for all observables, since, e.g., transport in quasicrystals is known to display "superdiffusive" behavior [11–13].

Finite-size effects and NFL behavior at finite temperatures.—To check the robustness of our scenario against finite-size effects, we performed simulations on approximants of different sizes N_a. For all approximants, we find a minimum Kondo temperature in the sample, T_K^{min}. Below T_K^{min}, FL behavior is then restored within our model (all local moments are screened). From Fig. 2, we learn that the power-law distribution of Kondo temperature $P(T_K) \propto T_K^{\alpha-1}$ emerges for $T_K < T_K^{typ}$. Taken together, these two observations imply, in principle, that the NFL range is restricted to the interval $T_K^{min} < T < T_K^{typ}$. However, our calculations show that T_K^{min} vanishes as N_a increases while T_K^{typ} remains finite. We thus conclude that

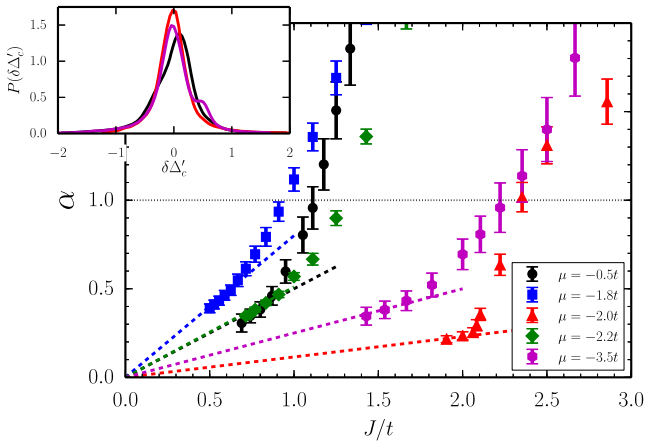

FIG. 3 (color online). Power-law exponent α as a function of the Kondo coupling J for five different positions of Fermi level μ. The dashed lines are linear fits deep into the Kondo regime where we expect $\alpha \propto J$ to hold (see text). The horizontal dashed line corresponds to $\alpha = 1$ and marks the entrance into the NFL region. At this point we have an average f-level occupation $\langle n_f \rangle = 1 - \langle Z \rangle = 0.970$, 0.995, 0.890, 0.995, and 0.960 for $\mu = -0.5t$, $-1.8t$, $-2.0t$, $-2.2t$, and $\mu = -3.5t$, respectively. Here we considered $N_a = 1393$ and $N_\phi = 576$. Inset: distribution of the real part of the local c-electron cavity function fluctuations at the Fermi level $\delta\Delta'_c = \Delta'_c(0) - \langle \Delta'_c(0) \rangle$ for three different values of μ (the color scheme is the same as in the main panel). Here we considered $N_a = 8119$ and $N_\phi = 64$.

the NFL range actually extends down to $T = 0$ in an infinite quasicrystal [29].

To access the finite-temperature behavior of the system and to observe the anticipated NFL behavior, we consider a simple interpolative formula for the local-moment susceptibility, $\chi(T, T_K) = 1/(T + T_K)$, which captures the leading behavior at both low and high-T [2,29]. We then calculate the magnetic susceptibility of dilute moments as an average of single-impurity contributions, $\langle\chi(T)\rangle = N_a^{-1}\sum_{\ell=1}^{N_a}\chi(T, T_K^{\ell})$, with sample results in Fig. 4 [54]. In the region $T \gg T_K^{\rm typ}$, $\langle\chi(T)\rangle$ shows the expected free-spin form for all values of the Kondo coupling. For $T \ll T_K^{\rm typ}$, and for $N_a \to \infty$, we observe two distinct behaviors depending on the value of α. For $\alpha > 1$ we recover the FL behavior at low-T with $\langle\chi(T)\rangle \sim 1/T_K^{\rm typ}$, whereas for $\alpha < 1$ we obtain $\langle\chi(T)\rangle \propto T^{\alpha-1}$. Moreover, in the crossover region, $T \sim T_K^{\rm typ}$, we have the surprisingly robust result $\langle\chi(T)\rangle \sim -\log(T)$, regardless of the value of α. This is due to the fact that $P(T_K)$ is essentially flat around $T_K^{\rm typ}$ (Fig. 2). For the smaller approximants, however, $T_K^{\rm min}$ is finite and hence FL behavior must be restored at $T < T_K^{\rm min}$ for all J. This is explicitly shown in the inset of Fig. 4 where $T_K^{\rm min} \simeq 10^{-2} T_K^{\rm typ}$ for $N_a = 7$.

Electronic Griffiths phase and $Au_{51}Al_{34}Yb_{15}$.—The Kondo-disorder(like) scenario discussed here nicely accounts for power-law divergences in the thermodynamic quantities when dilute Yb local moments are placed in a metallic quasicrystal. However, the quasicrystal $Au_{51}Al_{34}Yb_{15}$ forms a dense Kondo lattice, and one may wonder to what extent our scenario is relevant in this context. Based on analogies with disordered Kondo systems (where both the dilute-impurity case and the lattice case produce $P(T_K) \propto T_K^{\alpha-1}$ [19,51,55,56]), we then expect power-law distributions of Kondo temperatures and the corresponding NFL phenomenology for χ and C/T also for the lattice problem. In that case, the NFL region is known as an electronic quantum Griffiths phase and it has by now been observed in several disordered strongly correlated systems [57,58].

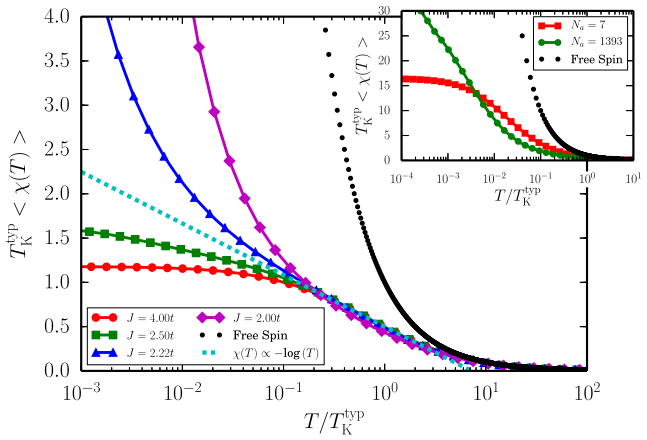

FIG. 4 (color online). Averaged value of the impurity susceptibility $\langle\chi(T)\rangle$ times the typical value of the Kondo temperature $T_K^{\rm typ}$ as a function of the temperature T normalized by $T_K^{\rm typ}$ for four values of the Kondo coupling J on a semilog scale. For completeness, we show both the free spin and the $\chi \propto -\log(T)$ $(\alpha = 1)$ curves. Here we considered $\mu = -2.0t$, $N_a = 1393$, and $N_\phi = 576$. Inset: $T_K^{\rm typ}\langle\chi(T)\rangle$ as a function of $T/T_K^{\rm typ}$ at $\mu = 2.2t$ and $J = 1.05t$ for two different approximant sizes: $N_a = 7$ and $N_a = 1393$.

The quasicrystal heavy fermion $Au_{51}Al_{34}Yb_{15}$ shows NFL behavior with $\chi \sim T^{-0.51}$, $C/T \sim -\log(T)$ [7] or $\chi \sim T^{-0.55}$, $C/T \sim T^{-0.66}$ [8]. Our results, however, predict the same NFL exponent for both χ and C/T, and this difference hampers a definite identification of quantum Griffiths effects [59]. On the other hand, the (Griffiths) power-law divergences are exact only at asymptotically low temperatures, where the regular contribution to the thermodynamic responses may be completely disregarded, and in general the results depend not only on the full form of the $P(T_K)$ curve but also on the particular shape of the scaling functions for the physical observables [29,54], which may account for differences in the exponent. One such example is the transient $-\log(T)$ divergence in $\langle\chi(T)\rangle$, which is present for all values of the exponent α in the region $T \sim T_K^{\rm typ}$, Fig. 4.

Interestingly, it was also reported that the temperature dependence of χ and C/T of the quasicrystal $Au_{51}Al_{34}Yb_{15}$ differs from that of its crystalline approximant. Reference [7] observes no NFL behavior for the approximant, whereas Ref. [8] does observe NFL behavior but with different powers as compared to the quasicrystal. To briefly address this intriguing result, we first notice that the size of the approximant unit cell considered in [7,8] is small and thus it is reasonable to assume that the experimental situation is similar to the one illustrated in the inset of Fig. 4, where the NFL behavior is bound to be observed only in a relatively narrow range $T_K^{\rm min} \lesssim T \lesssim T_K^{\rm typ}$. Moreover, due to the strong energy dependence of $\langle\rho_c(\omega)\rangle$, Fig. 1(c), especially for μ close to a dip (which seems to be case for $Au_{51}Al_{34}Yb_{15}$ [60]), tiny variations in parameters, such as the band filling or Kondo coupling, may drive the system to or from a NFL behavior. Therefore, care should be taken when drawing any conclusions from this distinct behavior.

Conclusions.—Motivated by the recently observed NFL behavior in the heavy-fermion quasicrystal $Au_{51}Al_{34}Yb_{15}$, we investigated the single-impurity Kondo effect in the octagonal (2D) and icosahedral (3D) tilings. We found a power-law distribution of Kondo temperatures $P(T_K) \propto T_K^{\alpha-1}$ and corresponding NFL behavior, in a surprising similarity to disordered metals. Therefore, a quasicrystalline conduction band provides a natural route to the emergence of a robust NFL behavior without the tuning of external parameters as doping, pressure, or external field.

For the Kondo quasicrystalline lattice problem, we expect, based on the analogy to disordered systems [17], a similar NFL behavior to be observed. In addition, it would be interesting to investigate the feedback effect of the local moments, in particular moments with $T_K < T$, on the transport properties of the quasicrystalline conduction electrons and the effects of intersite spin correlations [61].

We gratefully acknowledge help from M. Mihalkovic with approximants of the 3D icosahedral tiling. A. J. thanks P. Coleman for useful discussions on the quasiperiodic heavy fermion $Au_{51}Al_{34}Yb_{15}$. E. C. A. was supported by FAPESP (Brazil) Grant No. 2013/00681-8. E. M. was supported by CNPq (Brazil) Grants No. 304311/2010-3 and No. 590093/2011-8. M. V. was supported by the Helmholtz association through VI-521 and by the DFG Grants No. GRK 1621 and No. SFB 1143. V. D. was supported by the NSF Grants No. DMR-1005751 and No. DMR-1410132.

[1] N. W. Ashcroft and N. D. Mermin, *Solid State Physics*, 1st ed. (Thomson Learning, Toronto, 1976).
[2] A. C. Hewson, *The Kondo Problem to Heavy Fermions*, 1st ed. (Cambridge University Press, Cambridge, 1993).
[3] G. R. Stewart, Rev. Mod. Phys. **73**, 797 (2001).
[4] M. Brian Maple, R. E. Baumbach, N. P. Butch, J. J. Hamlin, and M. Janoschek, J. Low Temp. Phys. **161**, 4 (2010).
[5] P. Coleman, C. Pépin, Q. Si, and R. Ramazashvili, J. Phys. Condens. Matter **13**, R723 (2001).
[6] H. v. Löhneysen, A. Rosch, M. Vojta, and P. Wölfle, Rev. Mod. Phys. **79**, 1015 (2007).
[7] K. Deguchi, S. Matsukawa, N. K. Sato, T. Hattori, K. Ishida, H. Takakura, and T. Ishimasa, Nat. Mater. **11**, 1013 (2012).
[8] T. Watanuki, S. Kashimoto, D. Kawana, T. Yamazaki, A. Machida, Y. Tanaka, and T. J. Sato, Phys. Rev. B **86**, 094201 (2012).
[9] M. Kohmoto, B. Sutherland, and C. Tang, Phys. Rev. B **35**, 1020 (1987).
[10] H. Tsunetsugu, T. Fujiwara, K. Ueda, and T. Tokihiro, Phys. Rev. B **43**, 8879 (1991).
[11] H. Q. Yuan, U. Grimm, P. Repetowicz, and M. Schreiber, Phys. Rev. B **62**, 15569 (2000).
[12] U. Grimm and M. Schreiber, in *Quasicrystals—Structure and Physical Properties*, edited by H.-R. Trebin (Wiley-VCH, Weinheim, 2003), pp. 210–235.
[13] A. Jagannathan and F. Piéchon, Philos. Mag. **87**, 2389 (2007).
[14] G. T. de Laissardière and D. Mayou, C.R. Phys. **15**, 70 (2014).
[15] S. Watanabe and K. Miyake, J. Phys. Soc. Jpn. **82**, 083704 (2013).
[16] V. R. Shaginyan, A. Z. Msezane, K. G. Popov, G. S. Japaridze, and V. A. Khodel, Phys. Rev. B **87**, 245122 (2013).
[17] E. Miranda and V. Dobrosavljević, Rep. Prog. Phys. **68**, 2337 (2005).
[18] V. Dobrosavljević, T. R. Kirkpatrick, and B. G. Kotliar, Phys. Rev. Lett. **69**, 1113 (1992).
[19] E. Miranda, V. Dobrosavljević, and G. Kotliar, J. Phys. Condens. Matter **8**, 9871 (1996).
[20] P. S. Cornaglia, D. R. Grempel, and C. A. Balseiro, Phys. Rev. Lett. **96**, 117209 (2006).
[21] S. Kettemann, E. R. Mucciolo, and I. Varga, Phys. Rev. Lett. **103**, 126401 (2009).
[22] S. Kettemann, E. R. Mucciolo, I. Varga, and K. Slevin, Phys. Rev. B **85**, 115112 (2012).
[23] V. G. Miranda, L. G. G. V. Dias da Silva, and C. H. Lewenkopf, Phys. Rev. B **90**, 201101 (2014).
[24] D. Shechtman, I. Blech, D. Gratias, and J. W. Cahn, Phys. Rev. Lett. **53**, 1951 (1984).
[25] A. P. Smith and N. W. Ashcroft, Phys. Rev. Lett. **59**, 1365 (1987).
[26] E. S. Zijlstra and T. Janssen, Europhys. Lett. **52**, 578 (2000).
[27] A. Richardella, P. Roushan, S. Mack, B. Zhou, D. A. Huse, D. D. Awschalom, and A. Yazdani, Science **327**, 665 (2010).
[28] A. Rodriguez, L. J. Vasquez, K. Slevin, and R. A. Römer, Phys. Rev. Lett. **105**, 046403 (2010).
[29] See Supplemental Material at http://link.aps.org/supplemental/10.1103/PhysRevLett.115.036403, which includes Refs. [30–39], for a detailed description of our numerical approach, further information on the octagonal tiling, the derivation of an asymptotic expression for $P(T_K)$, and results for the 3D icosahedral tiling.
[30] A. Chhabra and R. V. Jensen, Phys. Rev. Lett. **62**, 1327 (1989).
[31] A. D. Mirlin, Phys. Rep. **326**, 259 (2000).
[32] G. Schubert, J. Schleede, K. Byczuk, H. Fehske, and D. Vollhardt, Phys. Rev. B **81**, 155106 (2010).
[33] F. F. Assaad, in *Quantum Simulations of Complex Many-Body Systems: From Theory to Algorithms*, edited by J. Grotendorst, D. Marx, and A. Muramatsu (John von Neumann Institute for Computing (NIC), Jülich, 2002).
[34] W. H. Press *et al.*, *Numerical Recipes: The Art of Scientific Computing*, 3rd ed. (Cambridge University Press, Cambridge, 2007).
[35] A. Jagannathan, Phys. Rev. B **61**, R834 (2000).
[36] D. S. Fisher, Phys. Rev. B **51**, 6411 (1995).
[37] T. Vojta, J. Phys. A **39**, R143 (2006).
[38] P. W. Anderson, Phys. Rev. **109**, 1492 (1958).
[39] E. Abrahams, P. W. Anderson, D. C. Licciardello, and T. V. Ramakrishnan, Phys. Rev. Lett. **42**, 673 (1979).
[40] As argued in J. Luck and D. Petritis, J. Stat. Phys. **42**, 289 (1986), the lower critical dimension for the existence of critical states in quasicrystals is 1D. In this sense, there should not be significant qualitative differences between electronic quasicrystalline states in 2D and 3D.
[41] J. E. S. Socolar, Phys. Rev. B **39**, 10519 (1989).
[42] D. Levine and P. J. Steinhardt, *The Physics of Quasicrystals* (World Scientific, Singapore, 1987).
[43] M. Duneau, J. Phys. A **22**, 4549 (1989).
[44] V. G. Benza and C. Sire, Phys. Rev. B **44**, 10343 (1991).
[45] C. Gros, Phys. Rev. B **53**, 6865 (1996).
[46] T. Rieth and M. Schreiber, Phys. Rev. B **51**, 15827 (1995).
[47] N. Read and D. M. Newns, J. Phys. C **16**, 3273 (1983).
[48] N. Read and D. M. Newns, J. Phys. C **16**, L1055 (1983).
[49] P. Coleman, Phys. Rev. B **29**, 3035 (1984).

[50] Because the $U \to \infty$ Anderson impurity model is particle-hole asymmetric, this definition of T_K is, in general, close but not equal to the onset temperature of a nontrivial solution ($Z_\ell \neq 0, \tilde{\varepsilon}_{f\ell} \neq E_f$) of the saddle-point equations.
[51] D. Tanasković, E. Miranda, and V. Dobrosavljević, Phys. Rev. B **70**, 205108 (2004).
[52] A. Clauset, C. R. Shalizi, and M. E. J. Newman, SIAM Rev. **51**, 661 (2009).
[53] V. Dobrosavljević and G. Kotliar, Phil. Trans. R. Soc. A, **356**, 57 (1998).
[54] Using this interpolative formula it is easy to see that $\langle \chi(T) \rangle = \int dT_K P(T_K)/(T + T_K) = \chi_r + \chi_s \cdot \chi_r$ is a regular contribution whereas $\chi_s \propto T^{\alpha-1}$ gives raise to NFL behavior for $\alpha < 1$ as $T \to 0$.
[55] E. Miranda and V. Dobrosavljević, Phys. Rev. Lett. **86**, 264 (2001).
[56] R. K. Kaul and M. Vojta, Phys. Rev. B **75**, 132407 (2007).
[57] E. C. Andrade, E. Miranda, and V. Dobrosavljević, Phys. Rev. Lett. **102**, 206403 (2009).
[58] M. C. O. Aguiar and V. Dobrosavljević, Phys. Rev. Lett. **110**, 066401 (2013).
[59] T. Vojta, J. Low Temp. Phys. **161**, 299 (2010).
[60] S. Jazbec, S. Vrtnik, Z. Jagličić, S. Kashimoto, J. Ivkov, P. Popčević, A. Smontara, H. J. Kim, J. G. Kim, and J. Dolinšek, J. Alloys Compd. **586**, 343 (2014).
[61] D. Tanasković, V. Dobrosavljević, and E. Miranda, Phys. Rev. Lett. **95**, 167204 (2005).